



Copyright © 2012, Paper 16-001; 46446 words, 10 Figures, 0 Animations, 3 Tables.
<http://EarthInteractions.org>

Flood Pulsing in the Sudd Wetland: Analysis of Seasonal Variations in Inundation and Evaporation in South Sudan

L-M. Rebelo*

International Water Management Institute, Addis Ababa, Ethiopia

G. B. Senay

U.S. Geological Survey Earth Resources Observation and Science Center, Sioux Falls,
South Dakota

M. P. McCartney

International Water Management Institute, Addis Ababa, Ethiopia

Received 1 October 2010; accepted 26 March 2011

ABSTRACT: Located on the Bahr el Jebel in South Sudan, the Sudd is one of the largest floodplain wetlands in the world. Seasonal inundation drives the hydrologic, geomorphological, and ecological processes, and the annual flood pulse is essential to the functioning of the Sudd. Despite the importance of the flood pulse, various hydrological interventions are planned upstream of the Sudd to increase economic benefits and food security. These will not be without consequences, in particular for wetlands where the biological productivity, biodiversity, and human livelihoods are dependent on the flood pulse and both the costs and benefits need to be carefully evaluated. Many African countries still lack regional baseline information on the temporal extent, distribution, and

* Corresponding author address: L-M. Rebelo, International Water Management Institute, P.O. Box 5689, Addis Ababa, Ethiopia.
E-mail address: l.rebelo@cgiar.org

characteristics of wetlands, making it hard to assess the consequences of development interventions. Because of political instability in Sudan and the inaccessible nature of the Sudd, recent measurements of flooding and seasonal dynamics are inadequate. Analyses of multitemporal and multisensor remote sensing datasets are presented in this paper, in order to investigate and characterize flood pulsing within the Sudd wetland over a 12-month period. Wetland area has been mapped along with dominant components of open water and flooded vegetation at five time periods over a single year. The total area of flooding (both rain and river fed) over the 12 months was 41 334 km², with 9176 km² of this constituting the permanent wetland. Mean annual total evaporation is shown to be higher and with narrower distribution of values from areas of open water (1718 mm) than from flooded vegetation (1641 mm). Although the exact figures require validation against ground-based measurements, the results highlight the relative differences in inundation patterns and evaporation across the Sudd.

KEYWORDS: Synthetic aperture radar; Wetlands; Inundation patterns; Evaporation; Flood pulse; Sudd

1. Introduction

Originating in Lake Victoria, the White Nile, one of the two major tributaries of the Nile River, flows from Uganda into South Sudan, where it enters a shallow depression and forms the vast Sudd wetland. Beyond the Sudd, the river flows to Khartoum, where it merges with the Blue Nile, forming the main stem of the Nile River, which subsequently flows through Egypt and into the Mediterranean Sea. Although wetland ecosystems occur extensively across the basin, from Lake Victoria in the south to the Nile Delta in the north, the swamps and floodplains of the Sudd constitute the largest wetland ecosystem in the Nile basin and one of the largest tropical wetlands in the world. The Sudd is dependent on the outflow from Lake Victoria but exhibits large seasonal changes as a consequence of variation in flow downstream of the lake. The “flood pulse concept” (FPC; Junk et al. 1989) describes the importance of the hydrological pulse to the functioning of wetlands and states that it is the annual inundation pattern that is primarily responsible for the high productivity of and the biotic interactions within such systems.

In addition to supporting high levels of biodiversity, the Sudd provides many other ecosystem services. It is estimated that more than 1 million people are almost entirely dependent on the wetland. The socioeconomic and cultural activities of the Nilotes living within and adjacent to the Sudd region are almost entirely dependent on the Sudd wetland (RIS 2006). It is a major source of water for domestic use and for livestock, and it is an important source of fish. The Sudd is one of the only water bodies of the Nile that is not overfished, and the potential yield (based on a surface area of 30 000–40 000 km²) has been estimated at 75 000 tons per year (Dumont 2009, 647–675). Many fish species migrate from the surrounding rivers to the nutrient-rich flood plains to feed and breed during the seasonal floods (Welcomme 1979). The socioeconomic and cultural activities of local people are dependent on the annual floods to regenerate the floodplain grasses, which feed their cattle. However, because of the protracted civil war in the region with the latest episode lasting from 1983 to 2005, very little is known about the current status of the biodiversity or the livelihood practices that are supported by the wetland.

The Comprehensive Peace Agreement (CPA), signed in 2005, ended 22 years of civil war, and in 2006 a core area of 57 000 km² of the Sudd was designated as a

Ramsar wetland site of international importance. Despite this status, recent discovery and extraction of oil in the Sudd threatens the diversity of the wildlife, aquatic macrophytes, and floodplains, as well as the hydrology of the intricate ecosystem (Springuel and Ali 2005). With the signing of the CPA, another major threat to the wetland is the completion of the Jonglei Canal. The original aim of the canal was to divert inflows to the Sudd in order to reduce evaporation from the wetland, thereby gaining approximately 4700 Mm³ of water for downstream use, as well as to reclaim approximately 100 000 ha of land for agriculture (Dumont 2009). Construction of the canal started in 1980 but was stopped by the onset of the civil war in 1983, after 260 of the total 360 km had been completed. In 2008, discussions to continue the work were resumed. If completed, the canal may have a significant impact on siltation and water quality; it may result in the loss of biodiversity, fish habitats, and important grazing areas, which all may have an effect on the livelihoods of the local populations (WWF 2010).

An understanding of the links between the hydrological pulse and the ecosystem is a prerequisite for deriving management plans for flood pulse wetlands such as the Sudd. Although it is known that the size of the Sudd varies substantially in response to seasonal and interannual changes in inflows, maps of recent flood extent and seasonal changes are unavailable for the total Sudd area and figures in the literature on the areal extent of the wetland vary considerably (Howell et al. 1988; Travaglia et al. 1995; Mohamed et al. 2004; Dumont 2009). This is due to variations in the definition of what constitutes the wetland, as well as differences in the approach used to map the area. In addition the area of wetland increased dramatically after the early 1960s because of increases in outflows from Lake Victoria. Different techniques have been applied to determine the size of the Sudd, including hydrological modeling (Sutcliffe and Parks 1999), thermal remote sensing (Travaglia et al. 1995), and a combination of hydrological modeling and remote sensing of evaporation (Mohamed et al. 2004). Although an area of 30 000–40 000 km² is frequently cited in the literature (Howell et al. 1988; Travaglia et al. 1995; Mohamed et al. 2004), figures range from approximately 7000 km² of permanent swamps to 90 000 km² of seasonal floodplain (Dumont 2009).

Because of the political instability in the region as well as the inaccessible nature of the Sudd, recent analyses have typically focused on the use of remote sensing datasets. Remote sensing technologies are essential in providing up-to-date spatial and temporal information about wetlands and their catchment basins and should be seen as a fundamental component in the development of wetland management plans for conservation and sustainable utilization (Rebelo et al. 2009). Although mapping of wetlands has proved difficult in many areas because of the lack of temporally and spatially consistent datasets, the systematic data acquisition strategy of new satellites such as the Advanced Land Observing System (ALOS) seek to redress this. The acquisition of data at a high temporal frequency is essential for the analysis of wetlands such as the Sudd, which are defined by seasonal flows.

Using a combination of recently acquired multitemporal and multisensor remote sensing datasets, the objectives of the research reported in this paper were to investigate and characterize flood pulsing of the Sudd wetland over a 12-month period. The time period chosen for the analysis was June 2007–May 2008 because of the availability of remote sensing data. Analyses of radar and optical remote sensing datasets are presented here to determine the spatial and temporal patterns of inundation within the Sudd and evaporation rates from the wetland during the 12-month period.

2. Characteristics of the Sudd region

2.1. Flood pulsing in the Bahr el Jebel

Flow in the Bahr el Jebel controls not only the hydrology but also many of the other biophysical characteristics of the Sudd (Dumont 2009, 334–364). At Mongalla, the point where it enters the Sudd, the river flow comprises outflow from the East African lakes (i.e., Victoria, Kyoga, George, Edward, and Albert), which is seasonally fairly constant but does fluctuate on a longer time scale, combined with locally generated and highly variable but unmeasured flow known as the torrents. The torrents are seasonal streams entering the Bahr el Jebel between Lake Albert and Mongalla. The torrents have steep basins and contribute spate flows as a result of local rainfall between April and October (Petersen et al. 2008).

From Mongalla, the Bahr el Jebel flows north, spreading laterally either side of the river. The Bahr el Jebel joins the Bahr el Ghazal (which enters from the west) at Lake No. Here, the combined river becomes the White Nile, although the contribution of flow from the Bahr el Ghazal is negligible in comparison to that of the Bahr el Jebel (Dumont 2009, 334–364). One of the rivers flowing through the Sudd is the Bahr el Zeraf, which flows out of the Bahr el Jebel north of Shambe and back into the White Nile downstream of Lake No (Figure 1). The northern limit of the Sudd is usually taken as the confluence of the White Nile and the Sobat Rivers at Malakal. Outflows from the Sudd (calculated as the difference between inflows at Malakal on the White Nile and the inflows from the Sobat River, measured just upstream of the confluence) are typically about half of the inflows, and the seasonal variation in inflow is damped out (Figure 2). Between 1907 and 1983,¹ the mean inflow was 33 180 Mm³ and the mean outflow was 16 135 Mm³. This includes the significant increase in flows following the jump in lake levels in Lake Victoria between 1961 and 1964 (Tate et al. 2004).

Rainfall over the Sudd is controlled by the movement of the intertropical convergence zone. Rainfall decreases slightly from southwest to northeast and varies considerably from year to year. Estimates of mean monthly rainfall derived as the arithmetic mean of gauges located within and just outside the wetland (i.e., Sutcliffe and Parks 1987) and using gridded datasets [i.e., Global Precipitation Climatology Centre (GPCC) and Tropical Rainfall Measuring Mission (TRMM)] indicate that mean annual rainfall is 870 mm (Table 1).

The inundated area of the Sudd varies both within and between years as inflow and rainfall varies. Annually, the maximum extent of flooding occurs after the rainy season (i.e., between October and December). It is estimated that the rise of Lake Victoria resulted in a trebling of the area of permanent swamp after 1964, with a smaller increase in the area of seasonal flooding (Sutcliffe and Parks 1999).

2.2. Site description

The total catchment area of the Sudd is nearly 1.48 million km² (Mohamed et al. 2005). Located between 6° and 9°8'N and between 30°10' and 31°8'E, the Sudd consists of a diverse range of habitats, which support a rich array of aquatic and

¹ Data records stopped in 1983 because of the onset of the civil war.

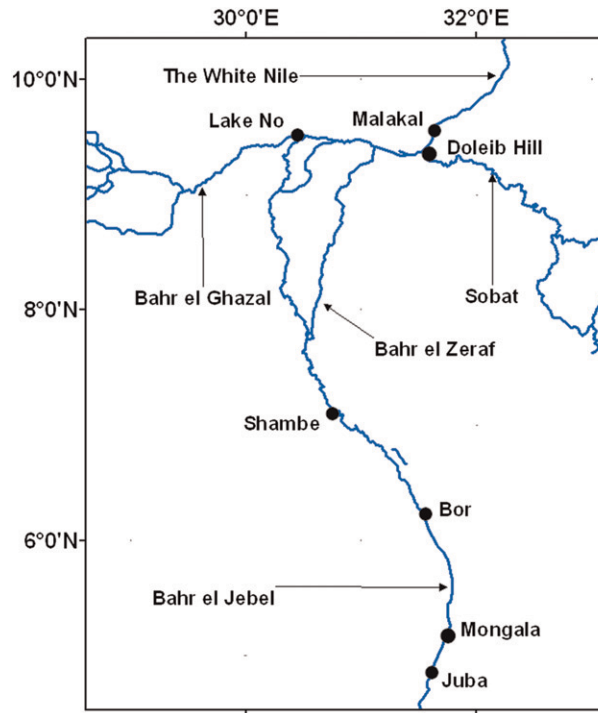


Figure 1. The Sudd region, South Sudan: river network and settlements.

terrestrial fauna (Rzóska 1974). Biodiversity within the Sudd is high, supporting over 400 bird and 100 mammal species. Located on the eastern flyway between Africa and Europe/Asia, the Sudd is one of the most important wintering grounds in Africa for Palearctic migrants, providing essential habitats for millions of migrating birds (Howell et al. 1988). During the 1980s the region was listed as supporting the highest population of shoebill storks (*Balaeniceps rex*) (East 1999) and the greatest numbers of antelopes in Africa (Stuart et al. 1990). Many of the antelopes undertake large-scale migrations across the Sudd, following the changing

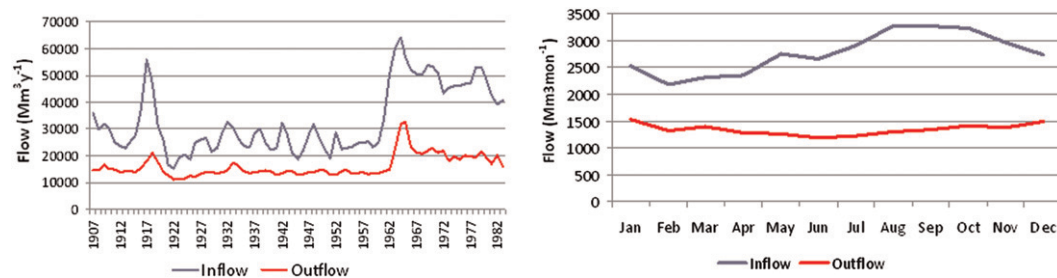


Figure 2. Inflow and outflow from the Sudd (1907–83): (a) annual time series and (b) mean monthly flow.

Table 1. Estimates of mean monthly rainfall over the Sudd (mm).

| | Period | Jan | Feb | Mar | Apr | May | Jun | Jul | Aug | Sep | Oct | Nov | Dec | Total |
|----------------------------|-----------|-----|-----|-----|-----|-----|-----|-----|-----|-----|-----|-----|-----|-------|
| Sutcliffe and Parks (1987) | 1941–70 | 2 | 3 | 22 | 59 | 101 | 116 | 159 | 160 | 136 | 93 | 17 | 3 | 870 |
| GPCC (gridded) | 1970–2007 | 1 | 2 | 14 | 46 | 101 | 116 | 143 | 157 | 123 | 83 | 16 | 2 | 805 |
| TRMM (gridded) | 1998–2008 | 3 | 3 | 15 | 51 | 105 | 123 | 146 | 185 | 166 | 113 | 31 | 7 | 948 |

water levels and vegetation. The wetland also has a high density and diversity of aquatic plants (Dumont 2009, 479–494).

Habitats within the Sudd region grade from open water and submerged vegetation to floating fringe vegetation, to seasonally flooded grasslands, to rain-fed grasslands, and finally to floodplain woodlands (Hickley and Bailey 1987). The core area of the permanent swamps is dominated by *Cyperus papyrus* with communities of *Phragmites communis* and *Vossia cuspidata*, bordered by stands of *Typha domingensis*. *Eichornia crassipes* (water hyacinth) is found along the open channels. Surrounding the permanent swamps are vast floodplains that consist of seasonally river-flooded grasslands (referred to locally as “toic”). These are estimated to cover an area of approximately 16 000 km² (WWF 2010) and are dominated by species of *Oryza longistaminata* and *Echinocloa pyramidalis*. An estimated 20 000 km² of rain-fed *Hyparrhenia rufa* grasslands surround the river floodplain (Robertson 2001). Beyond these are the floodplain woodlands, which are dominated by *Acacia seyal* and *Balanites aegyptiaca*.

Because the objective of the work was to characterize seasonal patterns of inundation and evapotranspiration (ET) from the Sudd, the study area was defined as the Bahr el Jebel contribution to the Sudd wetland, that is, excluding the neighboring Bahr el Ghazal swamps and the Sobat marshes. The Sudd area was determined by delineating the catchment for the main stem of the Bahr el Jebel between Juba in the south and the confluence with the Sobat in the north (see Figure 1).

3. Materials and methods

3.1. Site delineation

Delineation of the Sudd wetland is extremely difficult because of its dynamic nature as well as the presence of adjoining wetland systems. In this study, the area of interest was derived from elevation data and catchment boundaries. The boundaries were delineated using the digital elevation model (DEM) from the Shuttle Radar Topography Mission (SRTM) and standard processing steps using the Hydrological Data and Maps Based on Shuttle Elevation Derivatives at Multiple Scales (HydroSHEDS) GIS toolkit (Lehner et al. 2006). This process was followed to determine the catchment boundary immediately to the west of the Bahr el Jebel and the boundary to the east, which included the Bahr el Zeraf. There is some uncertainty about the contribution of the Bahr el Jebel to the wetlands of the Bahr el Ghazal on the northwestern edge of the Sudd, especially during high flows. However, this area was excluded from the analyses. The catchment of the Sobat was also excluded. The White Nile to the east of Lake No was assumed to mark the northern limit of the area of interest (Figure 1). The elevation at Juba (455 m on the SRTM digital elevation model) was used to define the southern boundary. The resulting study site is shown in Figure 3.

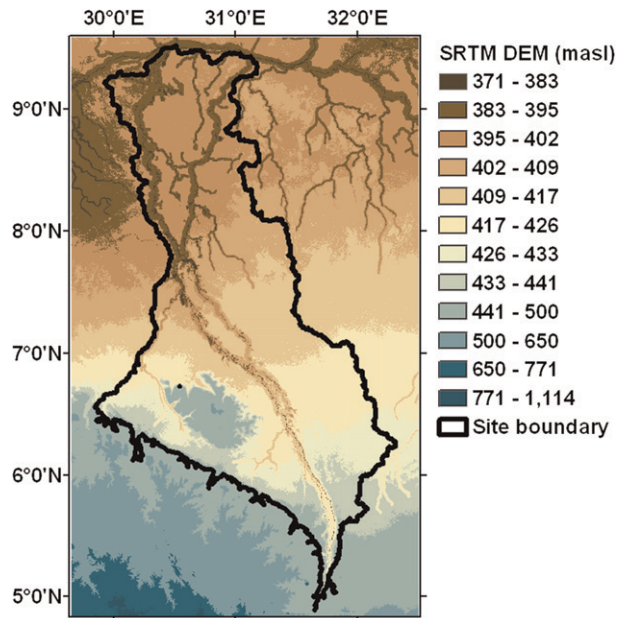


Figure 3. Elevation and site boundary of the Sudd, South Sudan.

3.2. Inundation patterns

Up-to-date maps of the Sudd wetland are not currently available. Because of the variable nature of inflows to the wetland and rainfall in the catchment, the area and extent of the wetland changes on an intra-annual as well as interannual basis. The seasonal variability and the lack of accurate information on the spatial extent of inundation for the region has led Mohamed et al. (Mohamed et al. 2004) to conclude that one of the major complexities in determining the regional-scale evaporation is the variability of the boundaries of the Sudd swamps. Although remote sensing datasets provide essential data for the characterization of inaccessible ecosystems, capturing the seasonal dynamics of tropical wetlands has proved problematic from high-spatial-resolution optical remote sensing data because of cloud cover during the period of maximum inundation (Rebelo 2010). In contrast, synthetic aperture radar (SAR) instruments have the capability to “see through” clouds and SAR data have been used successfully to map the extent and timing of inundation (Hess et al. 1995; Smith 1997). Within the framework of the Kyoto & Carbon (K&C) Initiative, the Japanese Aerospace Exploration Agency (JAXA) is focused on the provision of L-band (~ 25 -cm wavelength) SAR datasets from the Phased Array L-band Synthetic Aperture Radar (PALSAR) instrument on board the *ALOS* satellite, which can be used to assist in the global mapping and monitoring of wetlands (Rosenqvist et al. 2007; Rebelo 2010). Under the wetland theme of this initiative, multiple L-band SAR datasets with horizontally sent, horizontally received signal (HH) polarization and a pixel spacing of 70 m have been acquired between June 2007 and May 2008 for South Sudan (Figure 4). These data have been provided by JAXA Earth Observation Research Centre (EORC) for research

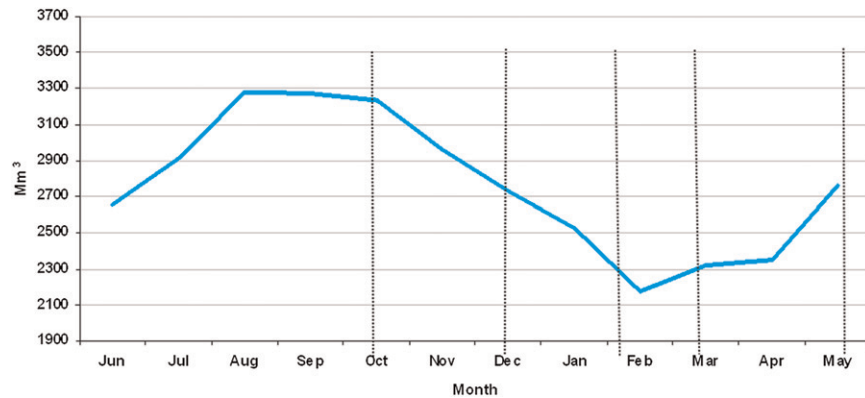


Figure 4. SAR acquisition dates (vertical dashed lines) and Sudd inflows (long-term mean 1907–83).

purposes within the framework of the K&C Initiative. The analysis of these is presented here to determine the spatial and temporal patterns of inundation within the area of interest.

Data processing

ALOS PALSAR data over the Sudd have been acquired at five time periods between June 2007 and May 2008: June 2007, September 2007, December 2007, February 2008, and May 2008. The PALSAR amplitude data were converted to normalized backscatter coefficients (σ^0) following Equation (1), where the digital number (DN) and the calibration coefficient (CF) are provided by JAXA (Shimada et al. 2009):

$$\sigma^0 = 10 \log_{10}(\text{DN}^2) + \text{CF}. \quad (1)$$

The data were filtered using a 3×3 median filter, followed by a 5×5 enhanced Lee filter, in order to reduce speckle and smooth areas of the image with similar ground cover (Lang et al. 2008). The Sudd wetland is located below 450 m MSL, where the Bahr el Jebel enters a shallow depression after flowing through the highlands. Areas above 455 m (SRTM DEM; Figure 3) were excluded from the analysis of wetland area because above this elevation the relief increases rapidly resulting in artifacts in the SAR data. Because these effects introduce error into the data and result in confusion between wetland and terrestrial classes, only pixels with an elevation less than 455 m were considered as potential wetland pixels.

The detection of open water and flooded vegetation from SAR data is well established, and time series of SAR images have been used successfully to map flood dynamics in different ecosystems (Rosenqvist and Birkett 2002; Hess et al. 2003; Martinez and Le Toan. 2007). The backscatter response from open water and from flooded vegetation at L band is well understood. The signal exhibits (i) high returns in areas of flooded vegetation due to the double-bounce effect as the radar signal is reflected off both the vegetation and the water surface, (ii) intermediate returns for dry land due to diffuse scattering from the ground and/or volume scattering

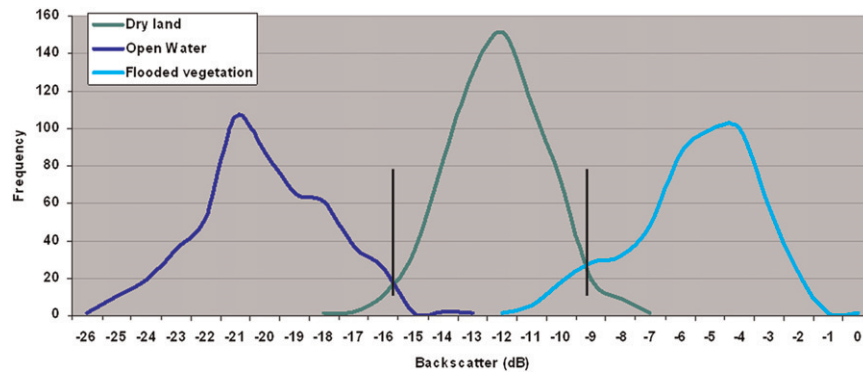


Figure 5. Frequency distribution of backscatter coefficients.

within vegetation canopies, and (iii) very low returns from open water due to specular reflectance (Wang et al. 1995; Toyra et al. 2002). Open water bodies and flooded vegetation have traditionally been detected in SAR images through thresholding, with class boundaries set through empirical evaluation of the image histograms (Ahtonen and Hallikainen 2005). This is the approach followed in this study, with threshold levels identified through histogram analysis. Although an absolute measure of soil moisture is not achieved, this approach provides a means of monitoring spatial and temporal changes in the hydrological state (Clark et al. 2009). The validity of applying empirically defined thresholds to SAR data to determine flooding and changes in the status of flooded areas, in particular in situations where it is not possible to acquire ground data, has been demonstrated by various authors (Melack and Wang 1998; van de Giesen 2000; Wang 2004). Flooded areas are often remote, and ground access may be extremely difficult. Access to the Sudd wetland has been further complicated during the last two decades by civil war.

Based on visual analysis and knowledge of the study area, backscatter coefficients for three classes (open water, flooded vegetation, and dry land) were extracted from the temporal sequence of images for areas that were temporally stable over the 12-month period. The histograms indicate a high level of separation between the three classes, with open water exhibiting very low returns, dry land exhibiting intermediate values, and flooded vegetation exhibiting high values (Figure 5). The horizontal lines show the selected thresholds with an upper value of -15 dB for open water and a lower value of -9 dB for flooded vegetation. The overlap between the histogram classes gives an indication of the errors associated with the threshold values.

3.3. Evapotranspiration

Monthly maps of actual evapotranspiration (ET_a) for the study area were generated using the Simplified Surface Energy Balance (SSEB) model (Senay et al. 2007) for the period between 2001 and 2009 (Figure 6). The SSEB model uses a combination of thermal datasets to develop ET fractions and reference ET (ET_o) generated using weather datasets from the National Oceanic and Atmospheric Administration (NOAA) Global Data Assimilation System (GDAS), as described

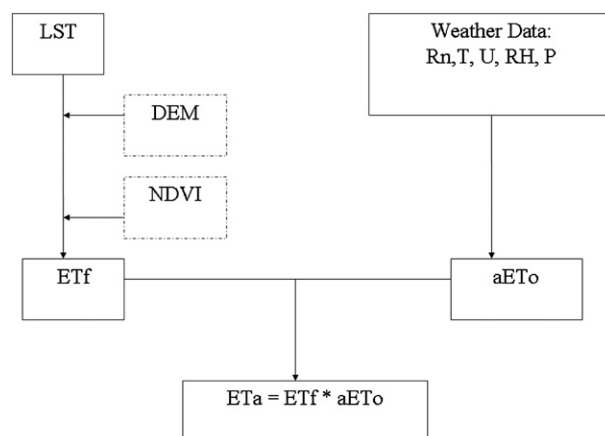


Figure 6. Schematic representation of the SSEB modeling setup.

in detail in Senay et al. (Senay et al. 2008). The land surface temperature (LST) is derived from satellite thermal data and suggested α is 1.2 when ETo is based on clipped grass reference ET. Net radiation is denoted as R_n , T is air temperature, U is wind speed, RH is relative humidity, and P is atmospheric pressure. The normalized difference vegetation index (NDVI) and DEM provide corrections to account for differences in land-cover and elevation-induced surface temperature changes, respectively.

The monthly ET data were calculated from 8-day estimates. The 8-day ET values were generated based on the 8-day-average Moderate Resolution Imaging Spectroradiometer (MODIS) thermal data and daily GDAS ETo. The 8-day total reference ET is multiplied with an average 8-day ET fraction derived from the thermal dataset. Monthly rainfall was generated for the same time period using satellite-based rainfall estimate (RFE; Xie and Arkin, 1997). The SSEB model has been validated using lysimeter data in the United States and has been shown to provide reliable estimates of ET. Statistical evaluation of results indicated that the SSEB accounted for 84% of the variability in the measured ET values (Gowda et al. 2009). The SSEB model with NDVI and topographic correction is documented in more detail in Senay et al. (Senay et al. 2010).

4. Results

4.1. Inundation patterns

The area of the Sudd and the components of open water and flooded vegetation vary considerably over the 12-month period. The lowest areas of open water are identified in September (4313 km²), whereas the highest expanse of flooded vegetation (27 186 km²) is also evident during this month. In contrast the greatest expanses of open water occur in December and January, when the area of flooded vegetation is lower. The monthly total area of wetland within the study site ranges from a minimum of 22 892 km² in June to a maximum of 32 701 km² in

Table 2. Seasonal variations in inundated areas (km²).

| Month/year | Open water | Flooded vegetation | Wetland |
|----------------|------------|--------------------|---------|
| June 2007 | 5850 | 17 042 | 22 892 |
| September 2007 | 4313 | 27 186 | 31 499 |
| December 2007 | 10 947 | 18 873 | 29 821 |
| January 2008 | 10 601 | 22 100 | 32 701 |
| May 2008 | 5365 | 19 892 | 25 257 |

January (Table 2). Note, however, that the latter figure does not refer to the total flooded area within the study site because different areas may flood at different times of the year.

The total area of the wetland, defined here as areas that were detected as either open water or flooded vegetation for any of the five dates during the 12-month period, is 50 510 km² (Figure 7). It should be noted that the flooding identified is not limited to river-fed flooding only but also to rain-fed flooding. Temporary flooding due to rainfall may occur locally in the rain-fed grasslands adjacent to the wetland (Hurst and Phillips 1938; Petersen and Fohrer 2010). Of the 50 510 km², 9176 km² constitutes the area of permanent swamps: that is, the locations where open water or flooded vegetation (Figure 7) is detected in each of the five dates during the 12-month period. The ratio of permanent to seasonal swamps is thus 18%, with the wetland area expanding to more than 4 times the size of the permanent swamps with the annual flood pulse and rainfall in the catchment.

4.2. ET over the Sudd

The ET varies substantially both spatially across the study site (Figure 8) and temporally over the 12-month period. Between June 2007 and May 2008, the estimated total ETa is 1449 mm, whereas the annual rainfall for the same period was 779 mm, meeting 54% of the ETa demand. The minimum ET occurs at the end of the dry period in April. The deficit ET months were August to April, with the maximum deficit occurring in December, with the lowest rainfall and a relatively high ET period.

Comparison of 2007–08 ETa to the full 9-yr dataset shows that 2007–08 had a similar temporal pattern but with a 10% higher ET than the mean year. This is probably caused by a higher rainfall in the region in the same period. The temporal variability of ET [coefficient of variation (CV) = 15%] is less than the temporal variability of the rainfall (CV = 60%). The peak ETa occurred in October for both the mean and the 2007–08 period. The peak rainfall during this period generally occurs from May to September. The fact that the ETa peak occurred right at the end of the rainy season makes sense because this is the period with less cloud (high energy) and with vigorous vegetation growth under unlimited water condition.

4.3. The relationship between inundation patterns and evaporation

In inaccessible wetlands, previous studies have typically used hydrological river stage data or other biophysical parameters where spatially explicit ground-based

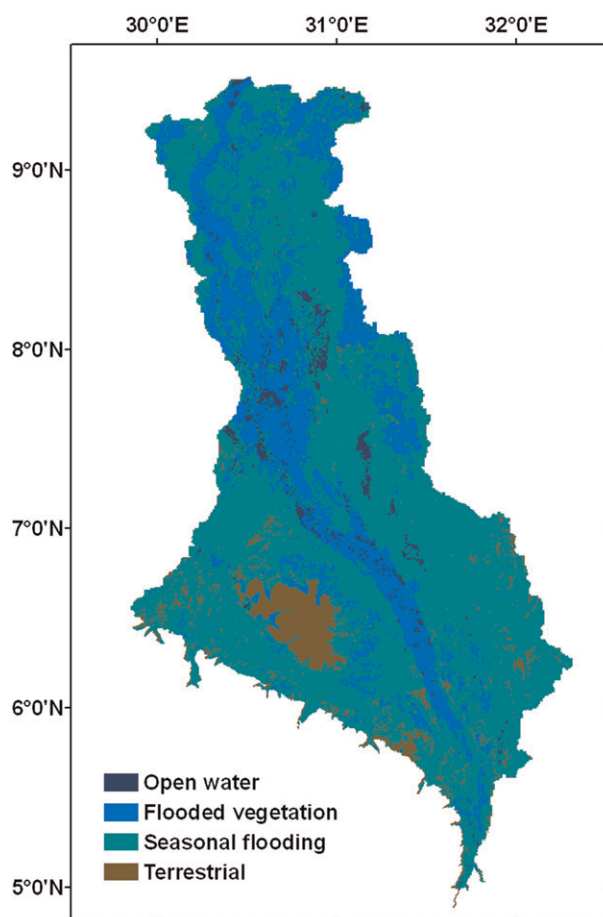


Figure 7. Spatial patterns of inundation (both river and rain fed), analyzed at five time periods between June 2007 and May 2008.

measurements of landscape condition are unavailable to validate the results (van de Giesen 2000; Rosenqvist and Birkett 2002). In the absence of ground-based measurements of inundation status, a statistical comparison has been performed (Figure 9) between the inundation results and ET, where the latter of which has been validated elsewhere (Gowda et al. 2009), for each of the 5 months that the area was mapped. There is a high level of agreement ($r^2 = 0.99$) between the area of wetland and the basin-average ET²; as the area of inundation increases based on the time of the year, so does the basin-average ET.

The maps of inundation status (i.e., open water or flooded vegetation) for the wetland at multiple time periods during a single year allow for the determination of mean annual ET values for different cover types. Mean ET values were calculated for areas of permanent wetland (i.e., pixels that were either classified as open water or flooded vegetation in *each* of the images: i.e., their status did not change during

² Basin refers here to the area of interest, which is defined as the Bahr el Jebel contribution to the Sudd.

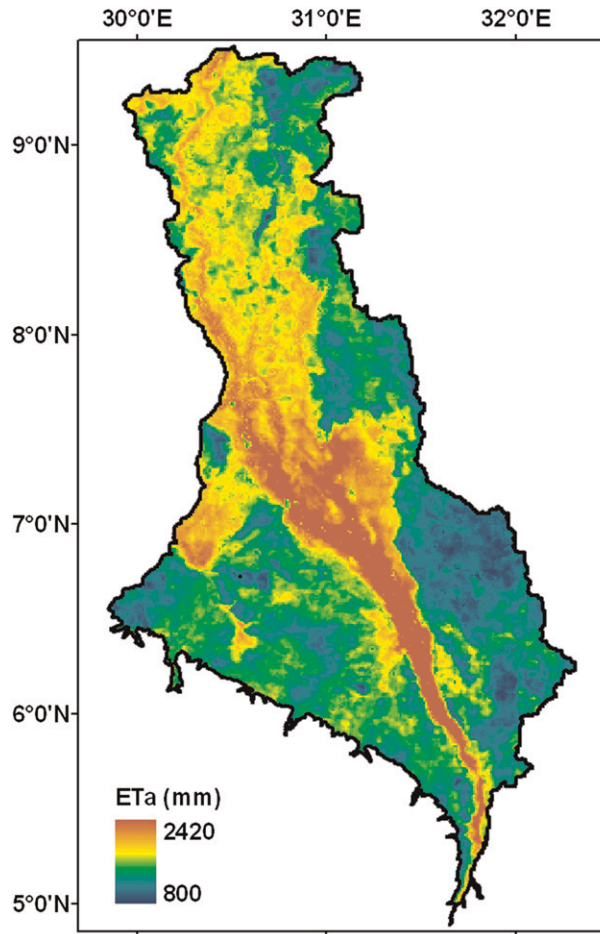


Figure 8. Total annual ETa (mm), June 2007–May 2008.

the 12-month period) as well as for the areas which were seasonally flooded (Table 3). The frequency distribution of the values for the permanent wetland is shown in Figure 10. It should be noted that, because of the different spatial resolutions of the two datasets (70 m for the wetland areas and 1 km for the ET), there may be mixing of values for pixels located at the boundaries of classes.

5. Discussion

Two parameters that are widely debated in the literature on the Sudd are the area of and the evaporation from the wetland. The former arises in part because of the use of arbitrarily defined boundaries for analysis of the wetland with the potential inclusion of neighboring systems and the use of different definitions as to what constitutes the Sudd. For the purpose of this study, the area has been defined based on topography and the drainage network, and the wetlands in the proximity of the Sudd (the Bahr el Ghazal swamps and the Sobat marshes) have been excluded.

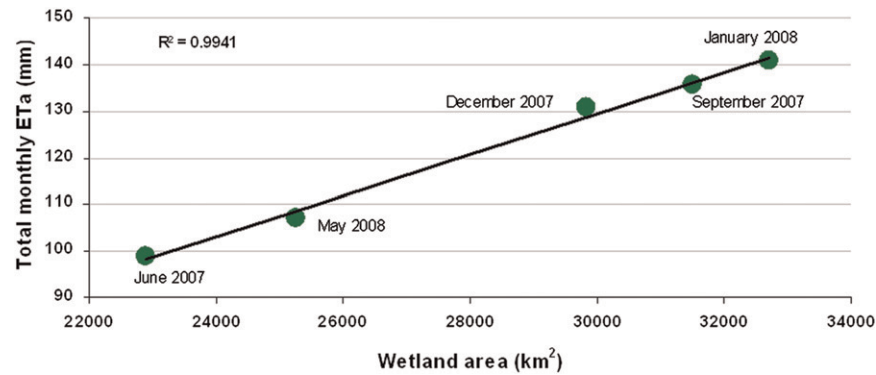


Figure 9. Comparison of monthly ET values and area inundated.

Within the defined study site, the total wetland area (50 510 km² of both river and rain-fed flooding) constituted 85% of the land surface between June 2007 and May 2008. Flooding in the Sudd wetland exhibits a distinct seasonal pattern that is determined by the level of the Bahr el Jebel and rainfall in the catchment. Although a core area of 9176 km² of permanent wetland was identified during the period June 2007–May 2008, at 41 334 km², the area of seasonal flooding over the 12 months was 4 times larger. The total wetland area is thus composed of 18% of permanent and 82% of seasonally flooded wetlands. The wetland was at its greatest expanse between September 2007 and January 2008 and at its lowest in June 2007 and May 2008, suggesting a 3–4-month lag following inflow at Juba and torrents in the catchment. This is in agreement with a remote sensing–based study by Travaglia et al. (Travaglia et al. 1995), which found that the wetland was at its greatest extent in December and January during the period December 1991–October 1992.

There is no consensus in the literature as to whether the evaporation from an open water surface is greater, the same, or lower than from a vegetated wetland surface under the same atmospheric and climatic conditions (Mohamed et al. 2012). Evaporation from the Sudd is a widely debated topic, with values varying from 1533 mm yr⁻¹ (Butcher 1938) to 2150 mm yr⁻¹ (Sutcliffe and Parks 1987) to 2400 mm yr⁻¹ (Migahid 1948). The largest discrepancy in previous studies seems to be whether to treat the wetland as open water or a vegetated surface, with most studies based on meteorological ground station data and the assumption that the area is permanently wet (Penman 1963; Sutcliffe and Parks 1999). Based on a theoretical approach using radiation, humidity, wind speed, and temperature, Penman (Penman

Table 3. Mean ET values for open water and flooded vegetation.

| | Total ET (Mm ³) | Mean ET (mm) | Area (km ²) |
|--------------------|-----------------------------|--------------|-------------------------|
| Open water | 1162 | 1718 | 692 |
| Flooded vegetation | 14 098 | 1641 | 8488 |
| Seasonally flooded | 59 763 | 1422 | 41 334 |
| Terrestrial | 9075 | 1311 | 6823 |

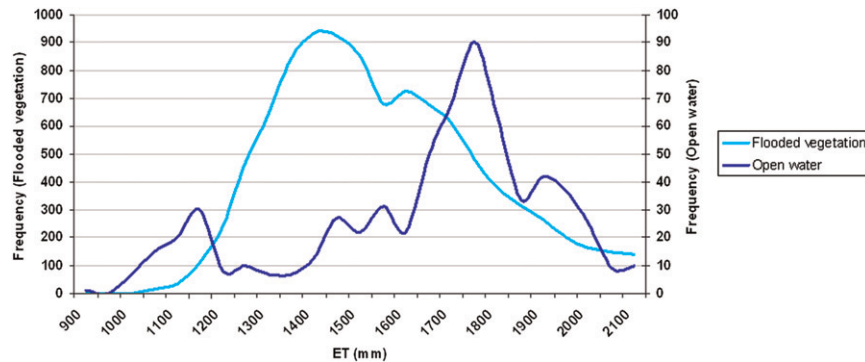


Figure 10. The frequency distribution of ET values for open water and flooded vegetation.

1948; Penman 1963) suggests that evaporation from dense wetland vegetation (papyrus) is the same as from open water. Sutcliffe and Parks (Sutcliffe and Parks 1987; Sutcliffe and Parks 1999) subsequently applied open water values of evaporation to investigate the water budget of the wetland. In contrast, the use of remote sensing allows for the spatial analysis of evaporation over a heterogeneous surface such as a wetland, which will be composed of a mosaic of open water bodies, emergent vegetation, and saturated soils. Recent work by Mohamed et al. (Mohamed et al. 2004) based on remote sensing–derived estimates of evaporation concluded that the values are site specific and are a function of the physical properties of the surface. Until now, detailed maps over a single annual season were not available describing the different components of the wetland. With the availability of the high-resolution maps of open water and flooded vegetation presented here for the permanent wetland area, as well as synergistic calculations of ET, it is possible to compare the derived values for each of the surface types. These values (Table 3) indicate that the mean annual ET from open water (1718 mm yr^{-1}) is indeed higher than that from flooded vegetation (1641 mm yr^{-1}). The mean annual value for the combined components (open water and flooded vegetation) is 1679 mm yr^{-1} , which is similar to the mean wetland value of 1636 mm yr^{-1} derived by Mohamed et al. (Mohamed et al. 2004). Although the mean values differ for open water and flooded vegetation, the range of values (Figure 8) is similar for the two cover types, suggesting that actual values vary with vegetation type and biophysical conditions.

Uganda, Ethiopia, and Sudan have ambitious plans for various dams along both the main stem of the Bahr el Jebel as well as its tributaries. The construction of these is already underway in some locations. In addition, it is not yet clear whether construction of the Jonglei canal will be resumed. Although these upstream developments may not reduce the flows to the wetland because they are intended for hydropower generation, they will have an effect on the seasonal flows into the Sudd. The data presented here show that the Sudd is an extremely dynamic wetland, the size of which varies greatly depending on the seasonal flood pulse.

Livestock are an essential component of the local economy, and it is the seasonally flooded areas that are of highest economic importance to the pastoral communities.

6. Conclusions

It has been emphasized in previous studies of the Sudd that one of the complexities in determining regional-scale evaporation has been the variability in the boundaries of and seasonal changes in the wetland (Mohamed et al. 2004). Despite the emphasis of Sutcliffe and Widgery (Sutcliffe and Widgery 1997) more than a decade ago of the need to investigate the natural regime of the wetland using satellite imagery to monitor the fluctuations with time, up-to-date maps of the spatial and temporal patterns of inundation within the Sudd were hitherto unavailable. Although mapping of tropical wetlands has proved problematic with the use of optical satellite images because of the presence of cloud cover at the time of maximum inundation, this study has mapped the seasonal changes in the Sudd wetland using radar remote sensing data, which are unaffected by cloud cover. The systematic acquisition strategy of *ALOS* PALSAR has enabled characterization of wetland dynamics at a high temporal resolution. Analysis of these data has provided high-resolution (70 m) maps of inundation patterns in the Sudd over the 12-month period June 2007–May 2008. Combining these with spatially explicit monthly calculations of ET over the Sudd has provided insights into variations in ET from the different wetland components.

The spatial variations and seasonal dynamics identified here emphasize the importance of the flood pulse to the Sudd wetland. Although temporal variations in inundation are the single most important factor in the formation and functioning of a wetland with small changes in the water regime having the potential to cause large changes in wetland functioning (Lang et al. 2008), future water resources developments in the region may result in the disruption of the timing and magnitude of the flood pulse. Although the exact figures presented require validation against ground-based measurements and should therefore be treated with caution, the results highlight the relative differences in inundation patterns and evapotranspiration across the Sudd over a 12-month period. Future work will extend the analysis over multiple flood cycles, in order to characterize the intra- as well as interannual flood dynamics of the Sudd and provide information that is crucial to the management of this vast resource.

Acknowledgments. This work has been undertaken within the framework of the JAXA Kyoto & Carbon Initiative and under the Nile Basin Focal Project (CP 59) of the Challenge Program on Water and Food. *ALOS* PALSAR data have been provided by JAXA EORC. All are gratefully acknowledged. Any use of trade, firm, or product names is for descriptive purposes only and does not imply endorsement by the U.S. government.

References

- Ahtonen, P., and M. Hallikainen, 2005: Automatic detection of water bodies from spaceborne SAR images. *Proc. IGARSS*, Seoul, South Korea, IEEE, 3845–3848.
- Butcher, A. D., 1938: The Sudd hydraulics. Ministry of Public Works, Cairo, Egypt Tech. Rep., 154 pp.

- Clark, R. B., I. F. Creed, and G. Z. Sass, 2009: Mapping hydrologically sensitive areas on the Boreal Plain: A multitemporal analysis of ERS synthetic aperture radar data. *Int. J. Remote Sens.*, **30**, 2619–2653.
- Dumont, H. J., Ed., 2009: *The Nile: Origins, Environments, Limnology and Human Use. Monographiae Biologicae*, Vol. 89, Springer, 818 pp.
- East, R., 1999: African antelope database 1998. World Conservation Union Species Survival Commission Occasional Paper 21, 454 pp.
- Gowda, P. H., G. B. Senay, T. A. Howell, and T. H. Marek, 2009: Lysimetric evaluation of the Simplified Surface Energy Balance approach in the Texas high plains. *Appl. Eng. Agric.*, **22**, 665–669.
- Hess, L., J. M. Melack, S. Filoso, and Y. Wang, 1995: Delineation of inundated area and vegetation along the Amazon floodplain with SIR-C synthetic aperture radar. *IEEE Trans. Geosci. Remote Sens.*, **33**, 896–904.
- , —, E. Novo, C. Barbosa, and M. Gastil, 2003: Dual-season mapping of wetland inundation and vegetation for the central Amazon basin. *Remote Sens. Environ.*, **87**, 404–428.
- Hickley, P., and R. G. Bailey, 1987: Food and feeding relationships of fish in the Sudd swamps (River Nile, southern Soudan). *J. Fish Biol.*, **30**, 147–160.
- Howell, P., M. Lock, and S. Cobb, Eds., 1988: *The Jonglei Canal: Impact and Opportunity*. Cambridge University Press, 537 pp.
- Hurst, H. E., and P. Phillips, 1938: *The Hydrology of the Lake Plateau and the Bahr el Jebel*. Vol. 5, The Nile Basin, Schindlers Press, 251 pp.
- Junk, W. J., P. B. Bayley, and R. E. Sparks, 1989: The flood pulse concept in river floodplain systems. *Can. Spec. Publ. Fish. Aquat. Sci.*, **106**, 110–127.
- Lang, M., E. Kasischke, S. Prince, and K. Pittman, 2008: Assessment of C-band synthetic aperture radar data for mapping and monitoring coastal plain forested wetlands in the mid-Atlantic region, U.S.A. *Remote Sens. Environ.*, **112**, 4120–4130.
- Lehner, B., K. Verdin, and A. Jarvis, 2006: HydroSHEDS technical documentation. World Wildlife Fund Rep., 27 pp. [Available online at http://gisdata.usgs.gov/webappcontent/HydroSHEDS/downloads/HydroSHEDS_TechDoc_v11.pdf.]
- Martinez, J.-M., and T. Le Toan, 2007: Mapping of flood dynamics and spatial distribution of vegetation in the Amazon floodplain using multitemporal SAR data. *Remote Sens. Environ.*, **108**, 209–223.
- Melack, J. M., and Y. Wang, 1998: Delineation of flooded area and flooded vegetation in Balbina Reservoir (Amazonas, Brazil) with synthetic aperture radar. *Verh. Int. Ver. Limnol.*, **26**, 2374–2377.
- Migahid, A. M., 1948: *Report on a Botanical Excursion to the Sudd Region*. Fouad I University Press, 159 pp.
- Mohamed, Y. A., W. G. Bastiaanssen, and H. H. Savenije, 2004: Spatial variability of evaporation and moisture storage in the swamps of the upper Nile studies by remote sensing techniques. *J. Hydrol.*, **289**, 145–164.
- , B. J. J. M. van den Hurk, H. H. G. Savenije, and W. G. M. Bastiaanssen, 2005: Impact of the Sudd wetland on the Nile hydroclimatology. *Water Resour. Res.*, **41**, W08420, doi:10.1029/2004WR003792.
- , W. G. M. Bastiaanssen, H. H. G. Savenije, B. J. J. M. van den Hurk, and C. M. Finlayson, 2012: Wetland versus open water evaporation: An analysis and literature review. *Phys. Chem. Earth*, doi:10.1016/j.pce.2011.08.005, in press.
- Penman, H. L., 1948: Natural evaporation from open water, bare soil and grass. *Proc. Roy. Soc. London*, **193A**, 120–145.
- , 1963: Vegetation and Hydrology. Commonwealth Agricultural Bureaux Tech. Communication 53, 124 pp.
- Petersen, G., and N. Fohrer, 2010: Flooding and drying mechanisms of the seasonal Sudd flood plains along the Bahr el Jebel in southern Sudan. *Hydrol. Sci. J.*, **55**, 4–16.

- , J. V. Sutcliffe, and N. Fohrer, 2008: Morphological analysis of the Sudd region using land survey and remote sensing data. *Earth Surf. Processes Landforms*, **33**, 1709–1720.
- Rebelo, L.-M., 2010: Eco-hydrological characterization of inland wetlands in Africa using l-band SAR. *IEEE J. Sel. Top. Appl. Earth Obs. Remote Sens.*, **3**, 554–559.
- , C. M. Finlayson, and N. Nagabhatla, 2009: Remote sensing and GIS for wetland inventory, mapping and change analysis. *J. Environ. Manage.*, **90**, 2144–2153.
- RIS, 2006: Information sheet on Ramsar Wetlands (RIS): The Sudd. RIS Key Documents of the Ramsar Convention 1SD002, 15 pp. [Available online at http://www.wetlands.org/reports/ris/1SD002_RISen06.pdf.]
- Robertson, P., 2001: Sudan. *Important Bird Areas in Africa and Associated Islands: Priority Sites for Conservation*, L. D. C. Fishpool and M. I. Evans, Eds., Birdlife International, 877–890.
- Rosenqvist, A., and C. M. Birkett, 2002: Evaluation of JERS-1 SAR mosaics for hydrological applications in the Congo River basin. *Int. J. Remote Sens.*, **23**, 1283–1302.
- , M. Finlayson, J. Lowry, and D. Taylor, 2007: The potential of long-wavelength satellite-borne radar to support implementation of the Ramsar Wetlands Convention. *Aquat. Conserv.*, **17**, 229–244.
- Rzóska, J., 1974: The upper Nile swamps, A tropical wetland study. *Freshw. Biol.*, **4**, 1–30.
- Senay, G. B., M. Budde, J. P. Verdin, and A. M. Melesse, 2007: A coupled remote sensing and Simplified Surface Energy Balance approach to estimate actual evapotranspiration from irrigated fields. *Sensors*, **7**, 979–1000.
- , J. P. Verdin, R. Lietzow, and A. M. Melesse, 2008: Global daily reference evapotranspiration modeling and evaluation. *J. Amer. Water Resour. Assoc.*, **44**, 969–979.
- , M. E. Budde, and J. P. Verdin, 2010: Enhancing the Simplified Surface Energy Balance (SSEB) approach for estimating landscape ET: Validation with the METRIC model. *Agric. Water Manage.*, **98**, 606–618, doi:10.1016/j.agwat.2010.10.014.
- Shimada, M., O. Isoguchi, T. Tadono, and K. Isono, 2009: PALSAR radiometric calibration and geometric calibration. *IEEE Trans. Geosci. Remote Sens.*, **47**, 3915–3932.
- Smith, L. C., 1997: Satellite remote sensing of river inundation area, stage, and discharge: A review. *Hydrol. Processes*, **11**, 1427–1439.
- Springuel, I., and O. M. Ali, 2005: Nile wetlands: An ecological perspective. *The World's Largest Wetlands: Their Ecology and Conservation*, L. H. Fraser and P. A. Keddy, Eds., Cambridge University Press, 448 pp.
- Stuart, S. N., R. J. Adams, and M. D. Jenkins, 1990: Biodiversity in Sub-Saharan Africa and its islands: Conservation, management and sustainable use. IUCN Species Survival Commission Occasional Paper 6, 242 pp.
- Sutcliffe, J., and Y. Parks, 1987: Hydrological modelling of the Sudd and Jonglei Canal. *Hydrol. Sci. J.*, **32**, 143–159.
- , and N. J. Wiggery, 1997: The problems of sustainable water resources management in Sudan. *Sustainability of Water Resources under Increasing Uncertainty*, IAHS Publication 240, IAHS, 259–265.
- , and Y. Parks, 1999: *The Hydrology of the Nile*. IAHS Special Publication. 5, IAHS Press, 179 pp.
- Tate, E., J. Sutcliffe, D. Conway, and F. Farquharson, 2004: Water balance of Lake Victoria: Update to 2000 and climate change modeling to 2100. *Hydrol. Sci. J.*, **49**, 563–574.
- Toyra, J., A. Pietroniro, L. Martz, and T. Prowse, 2002: A multi-sensor approach to wetland flood monitoring. *Hydrol. Processes*, **16**, 1569–1581.
- Travaglia, C., J. Kapetsky, and G. Righini, 1995: Monitoring wetlands for fisheries by NOAA AVHRR LAC thermal data. FAO/SDRN Rep., 30 pp.
- van de Giesen, N., 2000: Characterisation of West African shallow flood plains with L- and C-band radar. *Proc. Remote Sensing and Hydrology*, Santa Fe, NM, IAHS, 365–367.

- Wang, Y., 2004: Seasonal change in the extent of inundation on floodplains detected by JERS-1 synthetic aperture radar. *Int. J. Remote Sens.*, **25**, 2497–2508.
- , L. Hess, S. Filoso, and J. M. Melack, 1995: Understanding the radar backscattering from flooded and non-flooded Amazonian forests: Results from canopy backscatter modeling. *Remote Sens. Environ.*, **54**, 324–332.
- Welcomme, R. L., 1979: *Fisheries Ecology of Floodplain Rivers*. Longman, 317 pp.
- WWF, cited 2010: Saharan flooded grasslands (AT0905). World Wildlife Foundation. [Available online at http://www.worldwildlife.org/wildworld/profiles/terrestrial/at/at0905_full.html.]
- Xie, P., and P. A. Arkin, 1997: A 17-year monthly analysis based on gauge observations, satellite estimates, and numerical model outputs. *Bull. Amer. Meteor. Soc.*, **78**, 2539–2558.

Earth Interactions is published jointly by the American Meteorological Society, the American Geophysical Union, and the Association of American Geographers. Permission to use figures, tables, and *brief* excerpts from this journal in scientific and educational works is hereby granted provided that the source is acknowledged. Any use of material in this journal that is determined to be “fair use” under Section 107 or that satisfies the conditions specified in Section 108 of the U.S. Copyright Law (17 USC, as revised by P.L. 94-553) does not require the publishers’ permission. For permission for any other form of copying, contact one of the copublishing societies.
